

Do-it-yourself guide: how to use the modern single-molecule toolkit

Nils G Walter, Cheng-Yen Huang, Anthony J Manzo & Mohamed A Sobhy

Single-molecule microscopy has evolved into the ultimate-sensitivity toolkit to study systems from small molecules to living cells, with the prospect of revolutionizing the modern biosciences. Here we survey the current state of the art in single-molecule tools including fluorescence spectroscopy, tethered particle microscopy, optical and magnetic tweezers, and atomic force microscopy. We also provide guidelines for choosing the right approach from the available single-molecule toolkit for applications as diverse as structural biology, enzymology, nanotechnology and systems biology.

In late 1959 the visionary Richard Feynman gave his now classic talk suggesting that “there’s plenty of room at the bottom,” which forecast that in the future “we could arrange the atoms one by one the way we want them,” and that high-resolution microscopes would allow a direct look at single molecules in biological samples¹. Nearly 50 years later, this prediction has spawned the fields of nanotechnology and single-molecule microscopy. In the 1980s so-called scanning probe and near-field microscopes were developed that use sharp, nanoscale tips to image, probe and manipulate individual atoms or molecules^{2–4}. Pioneering efforts in the late 1980s and early 1990s realized optical single-molecule detection in wide-field microscopes^{5–8}. Although at first limited to the observation of single chromophores embedded in a crystalline matrix at low temperatures, imaging of single molecules under ambient conditions soon became possible^{9–11}, enabling the envisioned broad applications of single-molecule tools in biology.

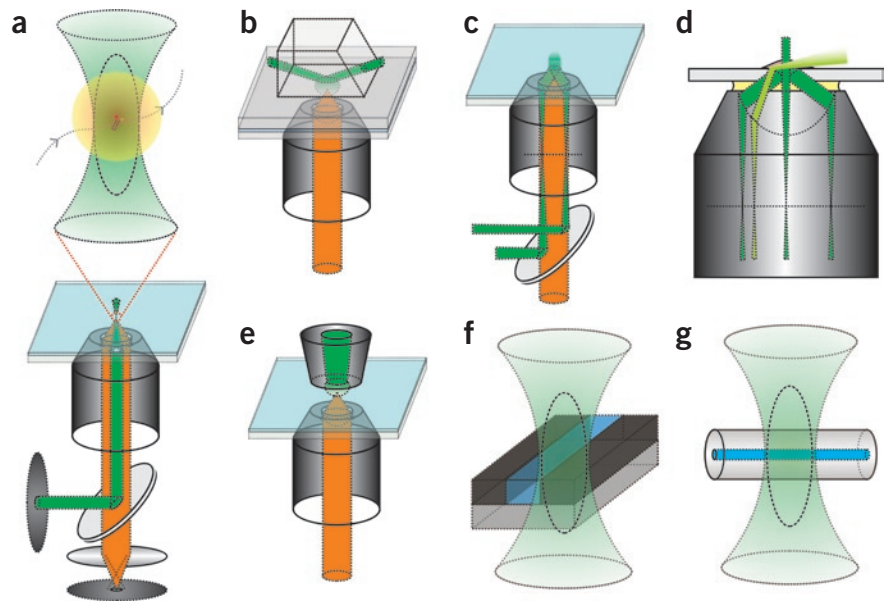
Many reviews have described the unprecedented insights into complex biological processes provided by the observation and manipulation of single molecules (for recent reviews see refs. 12–19). Briefly, according to the ergodicity hypothesis from statistical mechanics, a sufficiently long time-average (or a sufficient number of observations) from a single molecule is equivalent to a standard population-averaged snapshot, suggesting that, in principle, a single-molecule experiment contains all information of the molecular ensemble.

Additionally, single-molecule approaches: (i) reveal heterogeneity and disorder in a sample, albeit in a finite observation window (typically seconds to hours), which seem to contradict the ergodicity hypothesis but are commonplace in biological systems; (ii) afford precise localization (with nanometer accuracy) and counting of molecules (up to 10^5 molecules/ μm^2) in spatially distributed samples such as a living cell; (iii) work at the low numbers observed for most specific biopolymers (proteins, nucleic acids, polysaccharides) in a living cell (typically 1–1,000), eliminating the need for artificial enrichment; (iv) enable the quantitative measurement of the kinetics (microseconds to minutes) or statistics of complex biological processes without the need for a perturbing synchronization of molecules to reach a sufficient ensemble-averaged signal; (v) reveal rare and/or transient species along a reaction pathway, which are typically averaged out in ensemble measurements; (vi) enable the ultimate miniaturization and multiplexing of biological assays such as single-molecule sequencing²⁰; (vii) facilitate the direct quantitative measurement of mechanical properties of single biopolymers and their assemblies, including the forces (10^{-2} to 10^4 pN) generated by biological motors; and (viii) provide a way to “just look at the thing,” as Feynman suggested¹, as one can argue that seeing single-molecule behavior is believing. In combination, these features lead to the profound intellectual and scientific appeal of single-molecule tools and their imminent potential to revolutionize all

Department of Chemistry, Single Molecule Analysis Group, University of Michigan, 930 North University Avenue, Ann Arbor, Michigan 48109, USA. Correspondence should be addressed to N.G.W. (nwalter@umich.edu).

PUBLISHED ONLINE 29 MAY 2008; DOI:10.1038/NMETH.1215

Figure 1 | Simplified schematics of single-molecule fluorescence microscopes. (a) In wide-field epi-fluorescence microscopy, a laser (green) illuminates an area several micrometers in diameter and fluorescence (orange) from single molecules is detected through the same light path. In narrow-field epi-fluorescence microscopy, a pinhole (dashed disc) is additionally placed into the excitation path to reduce the excitation volume, therefore increasing the signal-to-noise ratio. In LCM and FCS, the excitation laser is focused to a diffraction-limited Gaussian beam waist. Pinholes are placed into both the excitation and emission paths (dashed discs), which greatly decreases the background from out-of-focus fluorescence and thus increases the vertical spatial resolution. In FCS single molecules usually diffuse into and out of the confocal ellipsoid, giving rise to stochastic fluorescence bursts (enlarged). (b) Prism-based TIRFM couples a laser beam into a prism above the critical angle to achieve TIR. (c) Objective-type TIRFM is created by moving the excitation laser beam from the optical axis of the objective to exceed the critical angle for TIR. (d) Close-up comparisons between epi-fluorescence microscopy (center light path), objective-type TIRFM and HILO microscopy (light green). (e) NSOM uses a glass fiber, drawn to a sharp tip, to optically probe single molecules on flat surfaces with a spatially constrained evanescent field that is smaller than the wavelength of light. (f,g) The space available to single molecules can be reduced by confinement in a microfluidic channel of smaller width than the diffraction limit (f) or in capillaries with inner diameters of 15–100 nm (g).



aspects of the biosciences including structural biology, enzymology, nanotechnology and systems biology. However, the capabilities of existing single-molecule techniques also have limitations, especially in the accessible measurement accuracies, time resolutions and time windows, as posed by the weak signal and potential for loss of the observed molecule.

Although many studies attest to the unique information gained from single-molecule observation (a conservative estimate places the number of relevant publications at ~2,000, with an exponentially increasing trend over the past four decades¹⁴), two bottlenecks have impeded an even more rapid and widespread incorporation of this approach into the biological sciences. The first bottleneck derives from the perceived requirement for expansive experience and expensive equipment. The accompanying review by Ha and coworkers seeks to encourage researchers to overcome this hurdle by building their own affordable single-molecule fluorescence microscope¹⁹. A complementary solution is the implementation of open-access resource centers, much like existing structural biology centers¹⁵, or other forms of collaborations with specialists. The second impediment to a broader application of single-molecule tools in biology stems from the need to identify the most suitable technique from the toolkit and develop the corresponding assay to solve the scientific question at hand. In this review we aim to provide practical 'do-it-yourself' guidelines for choosing the optimal single-molecule tool for any number of research problems. The best choice will depend on the observable of interest, so for several categories of observables we provide examples for successful single-molecule assays as well as a discussion of data analysis, limitations and possible future advances. First, however, we survey the rapidly expanding optical and force microscopy toolkit available to the single-molecule microscopist (electrophysiology techniques as applied to single membrane-bound ion channels are beyond our scope).

METHODS BASED ON OPTICAL OBSERVATION

An essential basis for making single-molecule observations is to dilute the molecule of interest to low (typically less than nanomolar) concentrations. The optical, mostly fluorescence-based, detection of single molecules has therefore been likened to finding the proverbial needle in the haystack, particularly if the signal-to-noise ratio is not carefully optimized^{21,22}. Several optical configurations stack the deck in one's favor and routinely achieve single fluorescent molecule sensitivity (Fig. 1 and Table 1). The basic components for these configurations are the microscope, light source(s), optical detector(s), probe(s) and sample²³.

Experimental configurations

Microscope designs. A microscope for single-molecule studies needs to efficiently reject background, such as autofluorescence as well as elastic Rayleigh and inelastic Raman scattering of the medium surrounding the target molecule, by optically isolating the desired Stokes- (red-) shifted fluorescence signal. A common way to decrease background while retaining signal is to decrease the excitation volume to where the molecule is expected, which can be accomplished by following four basic principles (Fig. 1).

First, the excitation volume can be confined using conventional optics. In wide-field epi-fluorescence microscopy the illumination and detection volumes are constrained by focusing light to illuminate an area several micrometers in diameter and using the same optics to detect fluorescence with an area detector. If desired, the excitation beam waist can be further narrowed with a 200–500 μm pinhole (narrow-field epi-fluorescence²⁴; Fig. 1a). Another approach, termed highly inclined and laminated optical sheet (HILO) microscopy (Fig. 1d and Table 1), uses a highly inclined beam near the objective edge that refracts into a thin optical sheet to penetrate the sample at a shallow angle²⁵.

Table 1 | Common terms in single-molecule microscopy

Term	Acronym	Technique description	Reference
Single-molecule fluorescence microscopy			
Burst-integrated fluorescence lifetime microscopy	BIFL microscopy	Uses a confocal geometry with time-correlated single-photon counting to detect photons with arrival times for lifetime measurements	34
Fluorescence (cross-) correlation spectroscopy	F(C)CS	Uses a confocal geometry to probe freely diffusing molecules by calculating the signal auto- (or cross-) correlation	44
Fluorescence intensity distribution analysis	FIDA	Similar to photon-counting histogram but with a more elaborate description of the excitation/detection volume	131
Highly inclined and laminated optical sheet microscopy	HILO microscopy	Uses a thin, laminated excitation sheet formed by displacing the excitation laser beam from the optical axis	25
Laser confocal microscopy	LCM	Uses a confocal pinhole to reject out-of-focus fluorescence and thus achieve a diffraction-limited focal detection spot that is raster-scanned over the sample	132
Near-field scanning optical microscopy	NSOM	Uses a sharp glass fiber tip to excite molecules with a spatially constrained evanescent field while raster-scanning over a surface	133
Objective-type total internal reflection fluorescence microscopy	OTIRFM	Uses an evanescent field generated at the interface by TIR through the microscope objective	28
Photon-counting histogram	PCH	Uses fluorescence brightness and concentration of the molecules to calculate the probability of observing m photons during integration time	134
Prism-type total internal reflection fluorescence microscopy	PTIRFM	Couples a laser beam into a prism above the critical angle to achieve TIR and generate an evanescent field at the interface	28
Ultra-high-resolution imaging techniques			
Fluorescence imaging with one-nanometer accuracy	FIONA	Localizes and tracks single-molecule emitters by finding the center of their diffraction-limited PSF	37
Nanometer-localized multiple single-molecule	NALMS	Uses a similar principle as single-molecule high-resolution imaging with photobleaching (see below) to measure distances between identical fluorescent probes that overlap within a diffraction-limited spot	54
Point accumulation for imaging in nanoscale topography	PAINT	Uses continuous specific or nonspecific binding of diffusing fluorescent probes to an object for high-resolution imaging	58
Photoactivatable localization microscopy	PALM	Serially photoactivates and photodeactivates many sparse subsets of photoactivatable fluorophores to produce a sequence of images that are combined into a super-resolution composite	56
PALM with independently running acquisition	PALMIRA	Records non-triggered spontaneous off-on-off cycles of photoswitchable fluorophores without synchronizing the detector to reach faster acquisition	112
Reversible saturable optical fluorescence transitions	RESOLFT	Generalized name for techniques such as STED and SPEM	115
Single-molecule high-resolution colocalization	SHREC	Two-color version of FIONA	52
Single-molecule high-resolution imaging with photobleaching	SHRIMP	Uses the strategy that upon photobleaching of two or more closely spaced identical fluorophores their position is sequentially determined by FIONA starting from the last bleached fluorophore	53
Saturated pattern excitation microscopy	SPEM	Wide-field technique that uses saturating standing-wave exciting light patterns together with the nonlinear dependence of fluorescence on the excitation intensity to make high-resolution information visible in the form of moiré fringes	135
Single particle tracking PALM	sptPALM	Combines PALM with live-cell single fluorescent particle tracking	114
Saturated structured illumination microscopy	SSIM	Alternative name for SPEM	136
Stimulated emission depletion	STED	Uses overlapping light beams to stimulate the surrounding emitters to reduce the effective focal detection spot in size	137
Stochastic optical reconstruction microscopy	STORM	Uses photo-switchable fluorophores to image a stochastically different sparse subset in each switching cycle and combine all images into a super-resolution composite	55
Force microscopy			
Atomic force microscopy	AFM	Uses a sharp tip mounted at the end of a flexible cantilever to image single molecules by raster scanning over a surface	3
Magnetic tweezers	MT	Uses an external magnetic field to exert force on a superparamagnetic bead that is tethered to a surface by a single molecule	71
Optical tweezers	OT	Uses light to exert force on a transparent bead that is tethered to a surface by a single molecule	59
Tethered particle microscopy	TPM	Tracks the Brownian motion of a microsphere tethered to a surface by a single molecule	61

Second, light from outside the focal volume can be eliminated using a small detection pinhole on the microscope side of the objective to keep out-of-focus light from reaching the detector (Fig. 1a). This method, called laser confocal microscopy (LCM), has several different implementations, as discussed elsewhere²⁶. In fluorescence correlation spectroscopy (FCS) and fluorescence cross-correlation spectroscopy (FCCS; Table 1), target molecules of one and two fluorophore colors, respectively, either freely diffuse through a fixed confocal volume or are immobilized²⁷, giving rise to stochastic fluorescence fluctuations that are temporally autocorrelated and cross-correlated, respectively, or otherwise statistically analyzed. Without immobilization the temporally autocorrelated molecules are not the same because new ones continuously pass through the confocal volume, leading effectively to ensemble averaging and a limited ability to interrogate or track individual molecules.

Third, total internal reflection (TIR) at a glass-solution (or quartz-solution) interface can be used to generate a standing wave ('evanescent field') that penetrates the solution to a depth of ~50–150 nm, depending mostly on the incident angle and relative refractive indices at the interface²⁸. Practical implementations of total internal reflection fluorescence microscopy (TIRFM; Table 1) use either a

quartz prism (Fig. 1b) or the microscope objective (Fig. 1c) to generate the evanescent field and illuminate surface-immobilized or surface-constrained molecules. The excitation beam paths for epifluorescence microscopy, HILO microscopy and objective TIRFM are relatively similar so that the same microscope can be switched between them (Fig. 1d). Finally, in near-field scanning optical microscopy (NSOM; Table 1), a metal-coated optical fiber with a tapered aperture of sub-wavelength diameter (~80 nm) generates a focused evanescent field that is scanned closely over a surface with immobilized target molecules and imaged using the same fiber or a high-numerical aperture objective (Fig. 1e). Although NSOM has found widespread applications in nanotechnology, it has proven difficult to apply to biological samples because of the need for a flat, stable sample surface and the fragility of the fiber tip.

Fourth, the detection volume can be physically restricted by, for example, using photophysics to silence neighboring molecules. More specifically, spatial resolution and signal-to-noise ratio are improved in stimulated emission depletion (STED) microscopy (Box 1 and Fig. 2) by depletion of out-of-focus fluorescent molecules or in photoactivated localization microscopy (PALM) and stochastic optical reconstruction microscopy (STORM) by stochastic photoswitching

BOX 1 SUPER-RESOLUTION IMAGING BY 'HARDWARE'-BASED METHODS

Reversible saturable optical fluorescence transitions (RESOLFT) techniques reduce the size of the point-spread function (PSF) by the use of sophisticated excitation configurations^{14,115}. Implementations include stimulated emission depletion (STED)^{115,131} and saturated pattern excitation microscopies¹³². In STED microscopy a diffraction-limited laser beam excites a focal sample volume and is followed (in pulsed STED) or accompanied (in continuous-wave STED¹¹⁷) by a donut-shaped stimulated emission beam that depletes the excited states of all fluorophores except those in the very center of the originally excited region (Fig. 2). Only molecules in the center of the focal volume remain in the excited state so that they are detected and imaged. Similarly to scanning laser confocal microscopy, the imaging beams are raster-scanned across the sample. The theoretical resolution limit of RESOLFT techniques is given by:

$$\Delta x, \Delta y \approx \frac{\lambda}{2\pi n \sin \alpha \sqrt{1 + I_{\max}/I_{\text{sat}}}}$$

where λ is the wavelength, α the semi-aperture angle of the lens, n the refractive index, I_{\max} the maximum of the light intensity outside of the center position and I_{sat} the light intensity to saturate the spectroscopic transition to be imaged¹¹⁵. This equation differs from Abbe's law by introducing I_{\max}/I_{sat} , which in principle can lead to infinite resolution, but at the cost of very high excitation intensities that may damage living cells or other light-sensitive samples.

Saturated pattern excitation microscopy^{132,133} or saturated structured illumination microscopy¹³³ is a wide-field, non-scanning super-resolution technique that projects excitation patterns on a fluorescent sample, rendering otherwise unresolvable high-resolution information visible in the form of low-resolution moiré fringes. Saturated structured illumination microscopy builds up higher resolution by using many different patterns¹⁴. Images require computational construction from the raw data, with the practical resolving power determined by the signal-to-noise ratio.

4Pi is a confocal fluorescence microscopy that increases the axial (z -axis) resolution of laser confocal microscopy by a factor of ~3–7 through the use of two opposing lenses with high numerical aperture to illuminate a single focal spot; the two wavefronts of the opposing beams interfere constructively at the focal point to narrow the focal maximum along the axial dimension. Interference of the spherical wavefronts above and below the focal plane creates side lobes in the image that are mathematically removed. I³M is a wide-field, nonconfocal method that implements the same opposing lens aperture enhancement in the detection of fluorescence but uses plane-parallel standing waves for excitation. Even though 4Pi and I³M are also 'hardware'-based methods that alter the PSF of the imaged fluorophore(s), they differ from the RESOLFT techniques, which rely on nonlinear effects from optical saturation of the emitters to shape the PSF.

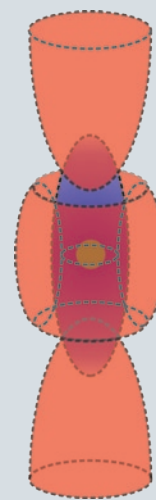


Figure 2 | STED narrows the PSF (blue) by depleting excited states around the very center of the excitation focus (orange).

of neighboring fluorophores (Table 1). Alternatively, a small nano-fluidic channel (Fig. 1f), capillary (Fig. 1g) or other compartment can be used to contain the target molecule in a volume smaller than the excitation volume, often in combination with other approaches to create a decreased excitation volume. In TIRFM, for example, the detection volume of single molecules can be physically further restricted by partially blocking the evanescent field with nanofabricated zero-mode waveguides^{29,30} or in partially etched optical fiber-bundle arrays³¹. Such physical containment strategies often lend themselves to integration with micro- and nanofluidic sample handling, which reduces the required sample volume and gives the opportunity to precisely control environmental conditions such as the timed release and mixing of reagents, fluid flow (shear force), and transient exposure to nanoscale manipulation and sensing devices³² (for a detailed discussion, see the accompanying review by Brewer and Bianco³³).

Light sources and optical detectors. In most cases lasers are used for single-molecule detection owing to their intense, coherent and collimated excitation light with well-defined wavelength. Lasers are either continuous or, if additional information such as an excited state lifetime is sought, pulsed³⁴. The most common detector for the single-point measurements performed in confocal fluorescence microscopy is the single photon-counting avalanche photodiode (SPAD or APD)²³ of nanosecond response time³⁵. A photomultiplier tube has a larger detection area, but offers lower quantum efficiency and requires higher operating voltage, which produces noticeable dark counts even when cooled²³. For detection of single molecules in a wide-field microscope, a specialized charge-coupled device (CCD) is the area detector of choice. A CCD camera does not count single photons *per se* but integrates photoelectrons over time with good quantum efficiency. The noise in each pixel of a cooled CCD chip does not notably increase with integration time, so longer integration leads to improved signal-to-noise ratio. Modern CCD cameras that reach single-fluorophore detection sensitivity with 1–100 ms integration times use image intensifier tubes with a photocathode, microchannel plate and phosphor screen (in an intensified CCD) or on-chip multiplication of photoelectrons (in an electron-multiplied CCD). The CCD imaging of the diffraction-limited spot of a single fluorescent molecule described in the implementation section below has recently become very popular because it enables measurement of the molecule's position at nanometer precision and can be used to visualize position changes over time that report on molecular-scale movement^{14,36–39}. The time resolution of a single fluorescent molecule detected by an APD is mostly limited by the photon count rate, which can be enhanced up to the excitation saturation level of the fluorophore at the expense of faster photobleaching, whereas detection by a CCD is primarily limited by the frame readout rate and quantum yield.

Probes. Fluorophores suitable for single-molecule detection fall into several categories: fluorescent organic dye molecules (including nonlinear optical chromophores), semiconductor nanocrystals also known as quantum dots, fluorescent proteins, fluorescent microspheres and gold nanoparticles. A suitable fluorophore needs to have: (i) high brightness, which is the product of the extinction coefficient of the fluorophore at the wavelength of excitation (should be $>20,000 \text{ M}^{-1} \text{ cm}^{-1}$) and the fluorescence quantum yield (ratio of emitted to absorbed photons) at the

wavelength of emission (should be $>10\%$); (ii) a relatively short excited-state lifetime (of a few nanoseconds) to quickly replenish the ground state; (iii) a large Stokes shift to facilitate rejection of scattered excitation light; and (iv) stable photophysical properties (rare photobleaching, low probability of dark states).

A widespread and powerful single-molecule fluorescence application is to measure intra- or intermolecular distances. For sensitive distance measurements by fluorescence resonance energy transfer (FRET) between two fluorophores, the detected distance(s) should fall within a range of 0.5- to 2-fold of the so-called Förster distance, which is the characteristic distance of half-maximal FRET efficiency of a specific fluorophore pair^{19,40}. To observe single fluorophore quenching by electron transfer, the electron transfer partner should be within a distance of $\sim 10 \text{ \AA}$. For a more in-depth discussion of the criteria for selecting fluorophores suitable for single-molecule measurements and strategies for their conjugation to a biopolymer see reviews by Kapanidis and Weiss⁴¹ and the accompanying review by Ha and coworkers¹⁹.

The sample. In single 'molecule' fluorescence microscopy the target may either be a covalently bonded molecule or a molecular assembly, which can be freely diffusing, spatially constrained or completely immobilized. Techniques that use an evanescent field for excitation and/or seek an extended observation time window require partial or full immobilization of the target molecule. Several approaches (discussed in ref. 42 and the accompanying review by Ha and coworkers¹⁹) have been successfully implemented to accomplish containment of the target molecule under conditions where it retains its native (solution-state) behavior. Recent additions to this arsenal are dielectrophoretic and electrokinetic trapping of freely diffusing molecules¹⁴. Which method is most suitable for a given problem depends on the stringency of surface passivation necessary to suppress nonspecific adsorption in the biological context.

Implementation and general considerations

Imaging. Both scanning and stationary modes of LCM can be used on spatially distributed biological samples, yet they yield different types of information. Scanning LCM can, for example, be used to obtain three-dimensional images of a live cell, but the quality of the image depends heavily on the scanning rate, which limits its ability to observe dynamic processes. 'Parking' an LCM focus on an imaged, immobilized biomolecule can then capture localized dynamic processes on a fast (microsecond) timescale. Spinning-disc confocal imaging uses a pattern of slits on a disk that spins at typically 3,000 r.p.m. to create virtual pinholes for confocal detection from a larger area⁴³. By comparison, confocal FCS analysis of diffusing molecules is suitable for determining the bulk concentration (nanomolar and below), diffusive properties and brightness as well as fast to intermediate dynamics (millisecond) and is limited by the photon count rate and focal residence time. New FCS detection schemes therefore aim to more directly access slower biological processes as well as higher target concentrations, whereas dual-color FCCS was developed to probe multiple components assembling into complexes^{44,45}. The spatial resolution of scanning LCM can be improved by incorporating 'hardware'-based high-resolution techniques (Box 1). Epi-fluorescence- and TIRF-based techniques are suitable to study intermediate to slow dynamics ($\geq 1 \text{ ms}$), limited by the CCD frame rate and image intensity requirements. In conjunction with 'software'-based high-resolution techniques,

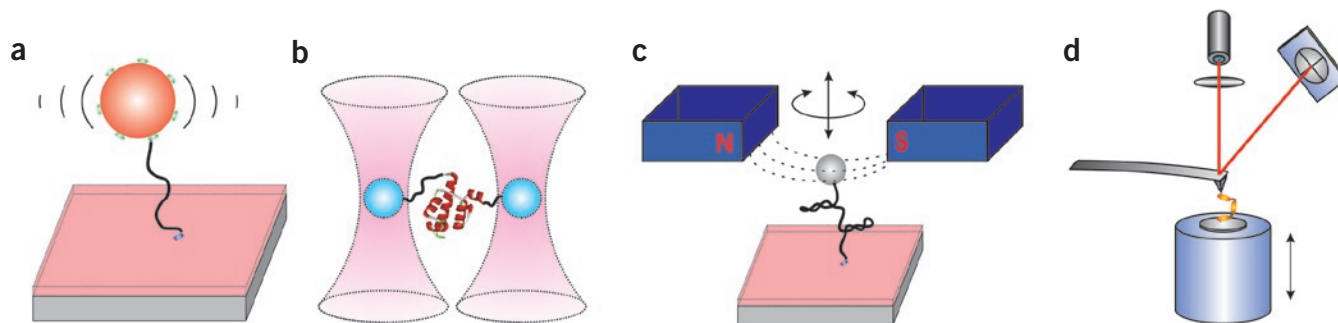


Figure 3 | Simplified schematics of single-molecule force microscopes. **(a)** Tethered-particle microscopy (TPM) monitors the restricted Brownian motion of an (often fluorescent) microsphere tethered to a surface by a single molecule. A directional force can be applied to the microsphere by a laminar solution flow. **(b)** Optical tweezers use light to levitate a transparent bead of distinct refractive index. The trapped bead is suspended at the waist of the focused (typically infrared) laser beam. The displacement of the bead from the focal center results in a proportional restoring force and can be measured by interferometry or back-focal plane detection. A single biopolymer can be suspended between two beads or a bead and a motorized platform. **(c)** Magnetic tweezers use an external, controllable magnetic field to exert force and/or torque on a superparamagnetic bead that is tethered to a surface via a single molecule. **(d)** AFM uses a sharp tip mounted at the end of a flexible cantilever to image single molecules bound on an atomically flat surface by raster scanning in the x - y plane (and often simultaneously tapping in the z dimension). AFM-based force spectroscopy exerts pulling force on a single attached molecule by retraction of the tip in the z direction. Cantilever bending is detected by the deflection of a laser beam onto a position-sensitive detector such as a quadrant photodiode. A piezoelectric actuator stage is used to control the positioning of the sample relative to the tip.

epi-fluorescence and TIRF have developed into valuable tools for *in vitro* and live cell imaging as well as particle tracking.

Single-particle localization and tracking. Many methods are available and are continuously being refined to allow biologists to probe the positions and distributions of particles in dynamic samples at high spatial and temporal resolutions, with wide-field optical microscopy as the major workhorse. Ernst Abbe intuitively postulated over 120 years ago that optical resolution is impossible below ~ 200 nm (referred to as ‘Abbe’s law’ or ‘Rayleigh’s resolution limit’)⁴⁶. Beginning in the late 1980s, however, light microscopy of fluorescent beads and metallic nanoparticles attached to biological specimens allowed the localization and tracking of features with spatial resolutions of tens of nanometers and time resolutions of tens of milliseconds, resulting in related techniques such as nanovid microscopy⁴⁷, single-particle tracking⁴⁸ and tethered-particle microscopy⁴⁹ (**Fig. 3**). As early as 1996, tracking of diffusive motions of membrane-constrained, dye-labeled single molecules was reported⁵⁰. A recent theoretical analysis showed that the resolution of optical microscopes is in fact not limited by Abbe’s law and can be improved by increasing the number of detected photons⁵¹. Current ultrahigh-resolution fluorescent microscopy tools can be classified either as techniques that use mathematical processing of the acquired diffraction limited image, in which the point-spread function (PSF) of an imaged fluorophore is analyzed using a priori knowledge about its shape (‘software’-based solutions, discussed below); or as techniques that take advantage of unique optical hardware configurations to suppress the PSF size through the use of specific sample illumination patterns¹⁴ (‘hardware solutions’; **Box 1**).

Recent ‘software’-based particle tracking of single fluorescent emitters has advanced to resolutions of up to 1.5 nm^{16,37}. Fluorescence imaging with one-nanometer accuracy (FIONA) localizes and tracks single-molecule emitters over time by finding the centers of their diffraction limited PSFs in a sequence of

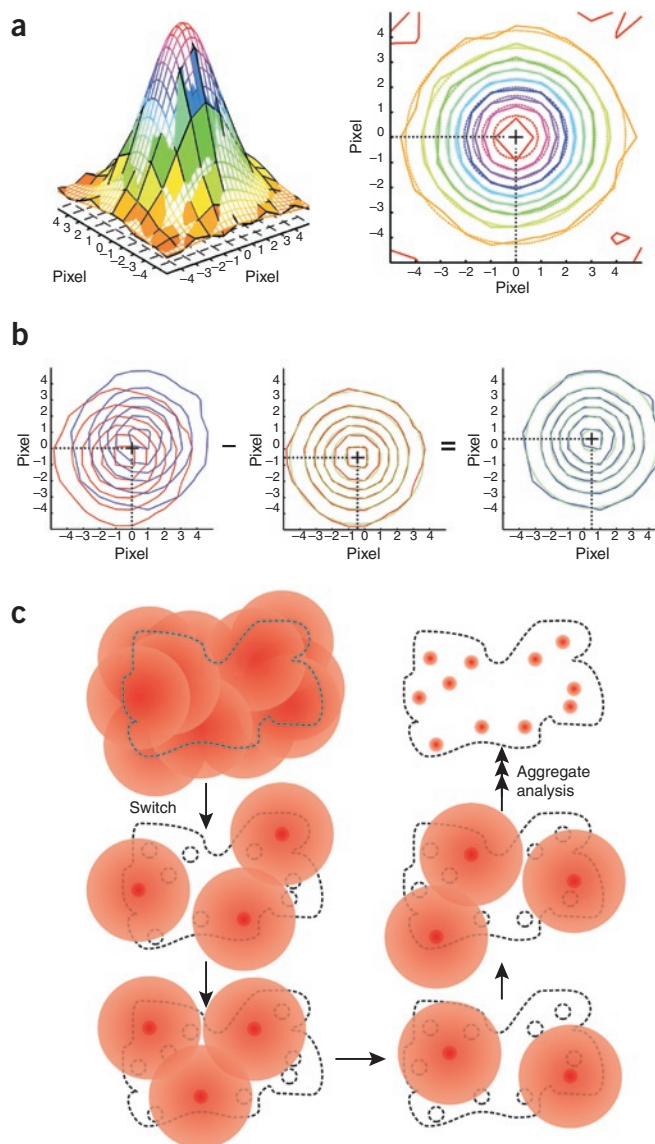
wide-field images. This is typically done by approximating the diffraction-limited Airy disk as a two-dimensional Gaussian function^{37,38} (**Fig. 4a**). Because fitting is a post-measurement, ‘software’-based manipulation of wide-field images, it can be applied in conjunction with a broad range of microscope configurations including TIRFM, epi-fluorescence microscopy and LCM. Most typically, images are recorded with a CCD and are thus pixilated. The accuracy with which the center position of a PSF can be localized is then given by the standard error of the mean:

$$\text{s.e.m.} = \sqrt{\frac{\sigma^2}{N} + \frac{a^2}{12N} + \frac{8\pi\sigma^4 b^2}{a^2 N^2}}$$

To first approximation, s.e.m. is the standard deviation (σ) of the Gaussian fit, divided by the square root of the total number of collected photons (N) (first term), revealing how important total photon count is for high accuracy. The effective pixel size of the camera, a , and the noise from background signal and detector, b , also have a role (second and third terms).

Multiple-particle localization and tracking. Several ultrahigh-resolution techniques build upon FIONA to expand their applicability to larger numbers of fluorophores. Single-molecule high-resolution co-localization (SHREC) is a two-color version of FIONA that uses fiduciary markers to measure the registration between two detection channels of separable spectral range⁵². Single-molecule high-resolution imaging with photobleaching⁵³ and nanometer-localized multiple single-molecule fluorescence microscopy⁵⁴ can be used to measure distances between identical fluorescent probes that overlap in a diffraction-limited spot. Upon stochastic photobleaching, the position of the last bleached fluorophore is determined by FIONA. This PSF is then subtracted from the previous image consisting of two overlapping PSFs from two proximal fluorophores, and FIONA is applied to define the PSF location in this difference image (**Fig. 4b**). This process may continue for an arbitrary number

Figure 4 | Ultrahigh-resolution imaging with ‘software’-based solutions. (a) The pixelized PSF of a single imaged fluorophore can be modeled by a two-dimensional Gaussian to determine its position with nanometer accuracy. The three-dimensional peak (left) shows the recorded intensity for each pixel as a colored surface, and the two-dimensional Gaussian intensity fit as a colored mesh. A corresponding contour map is shown (right). (b) Two fluorophores with a separation shorter than the diffraction limit can be individually localized by subtracting the PSF of one fluorophore from the initial overlapping image after the other fluorophore is photobleached or has adopted a dark state. (c) An aggregate reconstruction of images with many overlapping fluorescence emitters is possible from sub-images produced by either sequentially photoactivating and photobleaching or cyclically photoswitching sparse stochastic subsets of fluorophores.



of fluorophores, with decreasing precision of centroid localization of each additional dye molecule.

STORM⁵⁵ uses single photoswitchable fluorescent emitters that are turned on and off by excitation light sources. A stochastically different subset of proximal fluorophores is activated with each imaging cycle, allowing for a higher chance of sufficiently separated PSFs for FIONA-type localization (Fig. 4c). Similarly, in PALM⁵⁶ and fluorescence PALM (F-PALM)⁵⁷ sparse subsets of photoactivatable fluorescent protein molecules within a sample with a high density of such probes are photoactivated and subsequently bleached. FIONA is applied to each image, and the aggregate position information is assembled into an ultrahigh-resolution image with as many as 10^5 PSFs/ μm^2 and separations of localized molecules resolved to ~ 10 – 60 nm. Finally, point accumulation for imaging in nanoscale topography is based on continuous transient (specific or nonspecific) binding of low concentrations of otherwise freely diffusing single fluorophores to an imaged object; once bound and imaged, the fluorophores are bleached to repeat the process⁵⁸. The centroids of the PSFs from these transient fluorescent signals are determined by FIONA and used to assemble a composite image of relatively large objects such as unilamellar vesicles.

METHODS BASED ON MECHANICAL INTERACTION

The ability to apply force to or measure forces generated by a single biopolymer opens up new avenues for manipulating biomolecules and interrogating cellular processes^{12,17,18}. Three forms of force microscopy are commonly used to study single molecules (Fig. 3)—optical tweezers, magnetic tweezers and atomic force microscopy (AFM)—and are described in detail in the accompanying review by Neuman and Nagy¹⁸. In addition, we discuss a fourth technique, tethered-particle microscopy (TPM). These forms of microscopy share some common features including that they typically operate chromophore- (label-) free as they extend a long biopolymer between two attachment sites (handles).

Experimental configurations

Optical tweezers (also known as optical traps) have been developed since the 1970s (ref. 59) and use the radiation pressure exerted by a focused laser beam on an object (usually a transparent spherical bead) of distinct refractive index to levitate it (Fig. 3b). The equilibrium position of the bead is close to the center of the laser focus (a slightly downward displacement is due to scattered light). Any displacement from this equilibrium position will produce a restoring force proportional to the displacement (as in a linear spring). In magnetic tweezers, the optically transparent plastic bead is replaced

by a superparamagnetic bead that is controlled by magnetic forces (Fig. 3c). Magnetic tweezers are an intrinsic force clamp device because the magnetic field gradient exerts a constant force on the superparamagnetic bead owing to the small size of the bead compared to the magnet. An atomic force microscope uses a sharp tip mounted at the end of a flexible cantilever as a scanning probe or force transducer (acting as a linear spring) and can be operated in either an imaging or force mode. TPM (Fig. 3a) can be viewed as a related technique because the restricted Brownian motion of a biopolymer tethered bead is tracked over time by CCD-based video microscopy, and used to calculate spring constants and other mechanical properties of the tethering biopolymer⁶⁰ or to monitor changes in its length upon mechanical extension in a laminar flow^{61,62}.

Force generation. In optical tweezers, an applied force can be generated by either changing the intensity of the laser (the trapped bead experiences a force proportional to the gradient of

the laser intensity used to trap it) or displacing the trapped bead away from the equilibrium position (following Hooke's spring law). Permanent-magnet magnetic tweezers act like a constant force clamp. By contrast, in electromagnet magnetic tweezers the applied force can be varied by changing the current through the electromagnet. A force-mode AFM uses a flexible cantilever as a linear spring while pulling back from the surface to exert forces on a single molecule that is bound to the imaged surface and becomes physi- or chemisorbed to the tip (Fig. 3d). Finally, in TPM it is possible to apply defined forces to the tethered biopolymer by introducing laminar flow⁶³.

Single-molecule manipulation. In a typical optical tweezers experiment a single biopolymer is suspended between two beads or a bead and a flat surface (the latter is typically controlled by a motorized stage), and a force extension curve is measured as the biopolymer ends are pulled apart or, conversely, the biopolymer length changes during a biological process and the bead is displaced from the trap center. In addition to a linear force, magnetic tweezers can be used to apply controlled torsional twist (torque) on a single molecule by simply rotating the magnetic field. Optical tweezers have also been demonstrated to have the ability to apply torque to the sample using nonspherical trapped microparticles and linearly polarized trapping beams^{64,65}, although the implementation is not as straightforward as in magnetic tweezers. In AFM, the bending of the flexible cantilever is readily amplified and detected by deflection of a laser beam onto a quadrant photodiode to generate a force-extension curve.

The sample. In force spectroscopy, the biomolecule of interest usually needs to be tethered to a bead or other surface through specific binding or a covalent linkage. Therefore, the surface immobilization strategies used in optical microscopy are equally applicable in force spectroscopy. Surface attachment is simplified by the commercial availability of functionalized polystyrene beads, superparamagnetic beads and AFM tips^{12,17,18}. To sufficiently separate its two attachment sites, the target molecules often have to be extended with stiff handles (such as double-stranded DNA). Although nonspecific adsorption to the tip is to be avoided in AFM imaging to ensure minimal disturbance of the sample, it is often desirable and sufficient in AFM force mode as long as the adsorption is strong enough to withstand the applied force. The yield of single biopolymers properly suspended between the two surfaces for force measurements may have to be further increased by careful sorting of the obtained force-extension curves and/or biochemical protocols that minimize incomplete assembly or nonspecific binding.

Implementation and general considerations

AFM imaging. The bending of the flexible cantilever in the AFM imaging mode generates a surface contour map representing the morphology of the molecules. The surface density of single molecules as well as their surface contour map and changes thereof over time are directly available from such AFM images⁶⁶. Consequently, conformational changes resulting from ligand binding or complex formation can be detected⁶⁷. Owing to their often random surface binding, the shape of identical molecules in AFM images may vary notably from one another as well as from their solution structure so that proper controls and a shape classification scheme may be necessary. If desired, additional single-molecule properties can be measured

or manipulated using related techniques such as scanning electrochemical microscopy⁶⁸ and scanning tunneling microscopy⁶⁹.

Force measurement. Optical tweezers are arguably the most sensitive single-molecule tool for linear force and motion measurements. They can exert forces of 0.1–300 pN with high time resolution (down to 100 μ s). Dual-trap dumbbell optical tweezers have the lowest mechanical noise that can be reduced by passing the trapping laser beam through a gas of low refraction index such as helium. Ångström-level displacements can thus be measured in real time over long timescales from minutes to hours and at time resolutions as high as milliseconds^{12,70}. Magnetic tweezers are most suitable for measuring slow molecular processes that require both force and torque^{12,71}. Magnetic tweezers do not suffer from the sample heating and photodamage observed with optical tweezers, but they have limited spatial resolution (as low as only 10 nm compared to 0.1 nm with optical tweezers) and do not allow full three-dimensional manipulation. The applied linear forces can be 0.05–20 pN, with a torque of up to \sim 1,000 pN/nm, depending on the properties and dimensions of the paramagnetic bead attached to the biopolymer¹². The measurement of rotations and torque generation in biology with magnetic tweezers can be impeded by the rather large torque exerted by this method. AFM in the force spectroscopy mode can affect large forces, in the range of 10–10,000 pN, combined with large biopolymer extensions of 1–10,000 nm¹². This wide range of forces makes AFM suitable for probing ligand-receptor interactions as well as covalent bond strengths⁷². However, the high stiffness of the cantilever (10 – 10^5 pN/nm) results in a lower bound on the applied force and a force resolution limit of \sim 10 pN.

CHOOSING THE RIGHT TOOL

How does one choose a suitable technique from the bulging single-molecule toolbox? Given the substantial effort that goes into developing an assay to answer the biological question(s) at hand, careful consideration needs to be given to the possible choices and their individual scope and limitations. We present a flowchart to aid in making an initial choice (Fig. 5). Additional refinement requires a consideration of scope and limitations in the context of the desired observable(s) as well as examples of successful applications.

Measuring target molecule count (concentration)

Scope and limitations. Single-molecule assays can detect minute sample amounts and typically work at low (nanomolar and below) target concentrations, a feature that becomes critical when it is challenging or impractical to produce the larger quantities needed for ensemble experiments. The ability to precisely count the number of molecules present is one of the most immediate benefits of all single-molecule tools except for those focusing on mechanical properties.

The advantage of imaging and counting single molecules by AFM is that it is a label-free method because imaging is based on the physical interaction of a scanning stethoscopic tip with the sample. However, the target molecules need to be bound to a flat mica or glass surface, and it may be necessary to increase their molecular weight by attachment to a larger feature or handle, if they are otherwise too small (less than \sim 14 kDa) to be visualized⁷³. In addition to the surface density of molecules, basic information on their shape at nanometer resolution is readily obtained from an AFM image⁶⁶, although there is a substantial risk that the AFM tip mechanically perturbs the sample.

If at least one suitable intrinsic or extrinsic fluorophore is available, single-molecule fluorescence tools allow one to detect the number of target molecules both *in vitro* and in living cells. Recent reviews have dealt with strategies for extrinsic fluorescent probe attachment^{74,75}. Once that is accomplished, the most straightforward approach to detecting a target molecule is to let it diffuse through a confocal laser excitation volume and detect the resulting photon burst. The concentration of the target and its diffusion coefficient, and thus size, can be measured—provided that the focal volume is calibrated—by single-burst, photon-counting histogram or by autocorrelation analysis in FCS^{16,44,76,77}. Surface-constrained fluorophore-labeled molecules—for which constraints may be imposed through direct surface attachment or containment within a living cell (membrane)—can be counted in images obtained by LCM, epi-fluorescence microscopy, HILO microscopy, TIRFM and NSOM. Epi-fluorescence and HILO microscopies illuminate target molecules throughout an imaged cell, but TIRFM can only be used to image close to the cell surface. Epi-fluorescence microscopy can lead to limited detection sensitivity resulting from background signal from out-of-focus planes. In TIRFM, this limitation is overcome by only illuminating molecules within the evanescent field. In all cases where fluorophores are used care has to be taken not to underestimate the number of molecules present owing to photobleaching or transitioning into temporary dark states (blinking), or to overestimate the number because of the presence of unbound probe. Using statistical models to account for such artifacts, components in aggregates or subunits in complexes can be counted as the number of photobleaching steps to zero signal^{78,79}. Overcoming such limitations, a recently described scheme for *in vitro* label-free optical detection of single molecules uses a sophisticated surface-functionalized whispering-gallery silica microcavity to capture target molecules, resulting in a resonant wavelength shift⁸⁰. Microfluidic sample handling and particle trapping methods have the potential to be used to count small numbers of molecules in large volumes⁸¹. Although future developments are likely to provide more label-free tools for the detection of single molecules, fluorescence offers observables outlined in the following that are less likely to be replaced anytime soon.

Measuring intramolecular distances

Scope and limitations in biopolymer folding and conformational dynamics. The determination of intramolecular distances using FRET between a donor-acceptor fluorophore pair has found

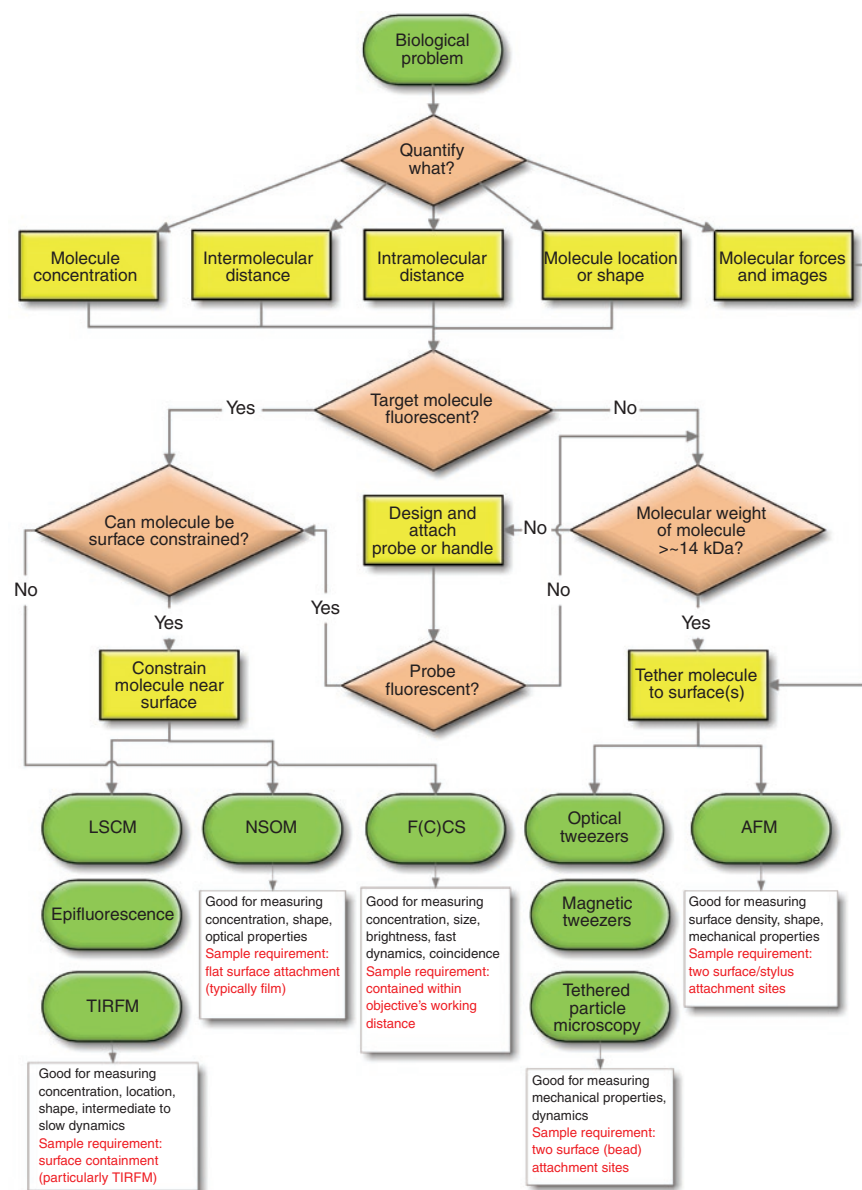


Figure 5 | Flowchart to select a suitable single-molecule technique to study a given biological problem.

widespread applications in structural biology to characterize the multidimensional conformational landscapes and dynamics of biopolymers^{12,13,16,82}. As a through-space interaction between two dipoles (the transition dipole moments of the two fluorophores), the efficiency of energy transfer falls off with a $1/(1 + (R/R_0)^6)$ dependence on the inter-dye distance R . The characteristic Förster distance R_0 ranges between 30 and 80 Å for most fluorophore pairs, making FRET a suitable biomolecular ruler at the low-nanometer scale²³. As discussed in the accompanying review by Ha and colleagues¹⁹, the single-molecule version of FRET can be used to quantitatively dissect the temporal sequence of events in folding transitions, including the adoption of rare and transient intermediates that may exist under either equilibrium or non-equilibrium conditions, which is rarely possible with ensemble-averaging techniques.

Single-molecule FRET measurements are performed on site-specifically doubly labeled proteins or nucleic acids that either are freely diffusing or are immobilized on carefully passivated glass or quartz surfaces. Absolute distances are difficult to calibrate⁸³, so that typically relative distance changes or differences are measured with a resolution of down to a few Ångströms¹⁹. Notably, opposite changes in donor and/or acceptor signal resolve biopolymer dynamics to an extent that is influenced by the finite averaging window of the time gated observation⁸⁴. A fast detector such as an APD in the single-point measurements of LCM or FCS is therefore optimal for observing conformational changes at the sub-millisecond and possibly nanosecond timescale, whereas a slower area detector such as a CCD camera can be used to observe more molecules in parallel and rapidly build reliable single-molecule statistics at millisecond time resolution. Processes slower than the detector resolution give rise to separate FRET histogram distributions, whereas faster processes lead to FRET signal averaging into a single distribution.

Fluorescence microscopy using single-pair FRET on surface-constrained or -trapped target molecules allows for the observation of structural dynamics over long periods of time. Time-lapse experiments with intermittent excitation can, in principle, preserve fluorophores over many hours before they photobleach. Control experiments need to be performed to ensure that the double labeling and immobilization of the target molecule has negligible effect on its biological properties. Although FRET is sensitive over a distance range of ~2–8 nm, photoinduced electron transfer (PET) reactions between an excited fluorophore and a redox-matched electron donor or acceptor can probe distances on the scale of a few Ångströms. This was demonstrated in the reversible electron transfer between flavin and a tyrosine residue in the catalytic core of a single flavin enzyme molecule, where a 1 Å distance change manifests in a several-fold change in flavin fluorescence lifetime and intensity⁸⁵. Several non-electron or non-energy transfer techniques have recently been used to study processes with slightly longer length scales (10–100 nm) that are not yet the domain of electron microscopy, among them the optical super-resolution techniques (**Box 1**) as well as the plasmon coupling of pairs of gold nanoparticles⁸⁶. Besides detecting internal motions, single-molecule FRET is also sensitive to changes in the rotational conformation as demonstrated by experiments on the ATP-dependent dynamics of F₁-ATPase⁸⁷.

Scope and limitations in enzymology. An enzyme's turnover rate often depends on conformational fluctuations. Conversely, conformational changes often accompany and facilitate enzymatic turnover. In these cases, single-molecule tools allow one to quantitatively dissect an enzymatic mechanism by monitoring the dwell times of diverse conformational states as defined by their FRET levels and/or dwell time constants^{13,88}.

Single-molecule enzymology where the enzyme is surface-immobilized and the substrate is diffusing, or vice versa, may be carried out using LCM, epi-fluorescence microscopy or TIRFM. The temporal resolution of LCM is bound in the lower limit by the time needed to detect a single photon and in the higher limit by the diffusion time of the sample molecule in the detection region, which can be expanded by (partial) sample immobilization. Epi-fluorescence microscopy or TIRFM can provide higher throughput as a result of observing a large number of molecules simultaneously.

Among successful examples for single-molecule enzymology are the experiments carried out on the small hairpin ribozyme, one of the simplest catalytic RNAs, to determine the multistep enzymatic reaction pathway¹³. Single-molecule probing in combination with mechanistic modeling⁸⁹, direct measurement of the dwell times associated with catalytic events⁹⁰ and kinetic fingerprinting by FRET⁹¹ have all been used to uncover the constituent elementary steps in the catalytic reaction. The challenges associated with these approaches naturally increase with the complexity of the enzymatic mechanism¹³.

Doubly labeling proteins site-specifically for single-molecule FRET is often difficult because of the limited number of labeling chemistries; complementary genetically encoded fluorophores of satisfactory photophysical properties for single-molecule detection are only slowly emerging^{74,75}. The problem is simplified for nucleic acid-binding motor proteins if the nucleic acid can be labeled, as has been the case, for example, in studies that dissected the mechanism of an RNA polymerase and a DNA helicase by confocal⁹² and TIR fluorescence microscopy⁹³, respectively. Most naturally occurring intrinsic fluorophores do not have sufficient quantum efficiency and/or photostability for current single-molecule detection tools. An exception is the enzyme cofactor flavin adenine dinucleotide (FAD) that has allowed Xie and coworkers to observe the conformational dynamics of single cholesterol oxidase molecules by monitoring the emission from the enzyme's fluorescent active site FAD⁹⁴. In a separate approach, a fluorogenic or fluorescent substrate may be used such that enzymatic action changes or localizes the fluorescence to a detectable extent^{29,95–97}. If multiple turnover is involved in the latter approach, successive products may have to be photobleached⁹⁶ or otherwise kept from saturating the detector²⁹. Single-molecule enzymology without the need for fluorophores but instead using force spectroscopy can be pursued if the substrate is a biopolymer such as a long DNA molecule whose length or helical twist is affected by the enzymatic reaction^{12,98}.

Scope and limitations resulting from heterogeneity. Since their introduction^{94,99,100}, single-molecule tools have often revealed heterogeneous behavior within a population of molecules, termed dynamic or static disorder (or memory), depending on the exchange rate between behaviors. A single enzyme molecule, for example, often exhibits large fluctuations of its folding and/or turnover rate constant at a broad range of time scales (from milliseconds to many hours^{88,96,101}). Such heterogeneity, which may or may not have biological relevance, is best delineated using single-molecule techniques, but makes the acquisition and sorting of large datasets a necessity to ensure statistical significance of the conclusions. One approach to increase the data richness of a single-molecule FRET experiment is to use three-color alternating-laser excitation, which allows for the simultaneous determination of three intramolecular distances¹⁰².

Measuring intermolecular distances

Scope and limitations. Self-assembly of macromolecular complexes is a process of fundamental importance in biology as well as much of modern nanotechnology. Most single-molecule tools that are suitable to measure intramolecular distances can also be applied to obtain intermolecular distances within complexes.

Successful applications of single-molecule tools to complex assemblies include studies of the signaling pathway involving the

calcium-binding protein calmodulin (CaM) by single-molecule FRET and fluorescence polarization using confocal microscopy¹⁰³. Moreover, the assembly of fluorophore-labeled tRNAs on immobilized ribosomes has been studied using FRET-based TIRFM⁹⁵. In these cases, double-labeling for FRET is facilitated because the interaction partners only need to be site-specifically labeled with one fluorophore each. Directed self-assembly, such as the hybridization of a complementary strand to an RNA molecule, can also be exploited using the site-specific attachment of fluorophores in cases where the assembly itself is not of interest^{104,105}. A careful choice of the labeling pattern usually depends on the system of interest. For example, attaching the donor to a DNA-binding protein in solution and the acceptor to its surface-immobilized DNA partner facilitates TIRFM detection of their interaction as a transition from negligible fluorescence signal to high FRET.

A 'holy grail' in biology is the quantification of molecular interactions in living cells, ideally at the single-molecule level, a challenge that only recently has started to be met. Dual-color FCCS can be used to detect two spectrally distinguishable, (ideally) non-interacting fluorophores within living cells in separate channels and cross-correlates their signals in real-time. FCCS therefore has been used to detect, for example, intracellular protein-protein and DNA-protein interactions without the need to measure actual distances^{44,106}. TIRFM¹⁰⁷ and spinning-disc confocal imaging⁴³ have been used to detect the association of membrane bound proteins in live and fixed cells, respectively, by single-molecule FRET. However, fluorophore labeling and rapid cellular diffusion are still the limiting factors for single-molecule studies of interaction partners in living cells⁴³. A recent approach has taken advantage of the slowed diffusion of a fluorescent protein-labeled transcription factor when bound to its (large) DNA target, as wide-field imaging with a long CCD integration time leads to localization enhancement of bound transcription factor and severe blurring of unbound transcription factor¹⁰⁸. Conversely, stroboscopic imaging can be used to virtually suppress diffusion of intracellular single molecules¹⁰⁹. Recently ultrahigh-resolution imaging techniques have provided independent access to the relative positioning, and thus information on the association, of interacting biopolymers.

Ultrahigh-resolution molecule localization

Scope and limitation in biological imaging. An ultimate goal in the biosciences is arguably to detect the dynamic positioning (and functional state) of each single molecule in a biological specimen¹⁵. Single-molecule imaging techniques such as FIONA are now capable of tracking biopolymers labeled with single organic dye fluorophores *in vitro* at low-nanometer precision and 1–500 ms time resolution^{14,38}. In living cells the resolution may be slightly lower, but single-molecule imaging holds the promise to reveal biological processes *in situ* and in real-time to reach a true systems-level understanding.

Single-molecule imaging resolution improves with the photon count, which can be enhanced by using longer detector integration times or brighter emitters such as quantum dots or nanoparticle scatterers. Quantum dots, for example, can be tracked in the sub-millisecond time range, even *in vivo*, but are often plagued by low labeling efficiency, large size and non-uniform shape, non-uniform excitation and emission characteristics, and blinking^{38,39}. Using two-color FIONA, or SHREC, a better than 10-nm distance between static fluorophores was determined¹⁵², and a real-time analysis of the tens-

of-nanometer steps of motor proteins on an immobilized substrate followed^{38,39}. SHREC uses the same setup as single-molecule FRET and hence can be applied in conjunction. Using single-molecule high-resolution imaging with photobleaching or nanometer-localized multiple single-molecule fluorescence microscopy analysis of sequential photobleaching events on static samples (Table 1), 10-nm distances between multiple identical fluorophores attached to a single target molecule (or complex) can be measured^{38,39}. These techniques allow for the localization of overlapping PSFs with similar spectral emission (that is, from identical fluorophores), but become more difficult and noisy with increasing photobleaching steps. As the analysis starts from the last photobleaching event, complete bleaching is necessary for the analysis, limiting the analysis to non-moving targets. Excitation intensities for any of these methods can be as low as a few W/cm², reducing photodamage in living cell samples. An application of these high-resolution imaging tools to nanotechnology has also been suggested¹¹⁰.

Stochastic imaging techniques are rapidly evolving. STORM gives very high resolution images (20–30 nm in the lateral and 50–60 nm in the axial dimension¹¹¹) as a result of the capacity to collect a large number of photons from each molecule, but is currently limited to the analysis of fixed samples because a reducing agent is required. By comparison, PALM and F-PALM are well-suited to studying living samples because they rely on fluorescent proteins, but presently available fixation methods may make them less suitable for analysis of fixed samples because of possible perturbation of fluorescence activity. Conventional PALM permanently bleaches each molecule after imaging, so each molecule is only counted once, whereas STORM, F-PALM and PALM with independently running acquisition (PALMIRA)¹¹² work by repeated activation and inactivation of probe subsets that may overlap with one another (Fig. 4c). PALMIRA thereby achieves ~100-fold faster collection times compared to PALM and, in combination with its single excitation laser requirement for activation and readout of the probes, results in lower background noise without the need for using TIRF imaging and preparing thin samples¹¹². Two-color PALMIRA has successfully been used to image an intracellular microtubule network of whole fixed cells at image acquisition times of 40–60 s and position precisions of 10–15 nm, showing that two-color imaging and protein colocalization in cells is possible with precision on the macromolecular scale¹¹³. The stochastic imaging technique combining single-particle tracking and PALM has been used to image membrane proteins at 20 frames/s in living cells, to map single-molecule diffusion of up to thousands of molecules in the plasma membrane and to create a spatially resolved map of single-molecule diffusion coefficients¹¹⁴.

An orthogonal approach to reaching ultrahigh resolution (often collectively referred to as super-resolution techniques) is to shape the PSF through the nonlinear effect that space-selective saturation has on emitter molecules surrounding the center of the excited region^{14,115}. It is expected that in the future the resulting 'hardware'-based ultrahigh-resolution techniques, generalized as reversible saturable optical fluorescence transitions (RESOLFT; Table 1 and Box 1), will be applied to a greater extent to single molecules. RESOLFT techniques such as STED (Table 1 and Box 1) can be used to image dynamical processes with ~20 nm resolution, even at two colors^{116,117}. The combination of STED with 4Pi microscopy (Table 1 and Box 1) is expected to further improve resolution in the axial dimension, and parallelization with multiple foci will allow larger areas to be examined faster¹¹⁵. Suitable combinations of both

'hardware'- and 'software'-based techniques may be envisioned to ultimately yield real-time measurements of the dynamic locations and nanoscale distances of large ensembles of single molecules, with broad applications in complex mixtures including living cells.

(Un)folding of target biopolymers

Scope and limitations. Single-molecule force manipulation and measurement techniques have been recognized as uniquely effective tools for characterizing the forces and motions that biopolymers can affect or withstand^{12,18}. The reconstruction of folding free energy landscapes of biopolymers is one focus of single-molecule force spectroscopy^{12,18}. Inter- and intramolecular interactions such as the unfolding of proteins and nucleic acids, the dissociation of molecular complexes and even the breaking of single chemical bonds can be induced and characterized through external mechanical force. The application of force along a specific (un)folding direction enforces a defined reaction pathway and can be related to the reversible work done (the free energy change), even under partially irreversible conditions, by repeatedly performing both folding and unfolding reactions and applying the Crooks fluctuation theorem to the observed work distributions¹¹⁸.

For such applications, available tools include optical tweezers, magnetic tweezers, AFM and flow-extension TPM (**Fig. 3** and **Table 1**), which can be used to measure conformational changes on length scales both larger and smaller than FRET. In addition, they can be applied when labeling with fluorophores is challenging or not feasible. Force is transduced through a biopolymer-tethered dielectric or magnetic bead in the case of optical tweezers, magnetic tweezers

and TPM or through the AFM tip. Tight specific attachment of the biopolymer to its force transducer and suppression of nonspecific binding are important requirements for force spectroscopy.

AFM is often used to unfold proteins with tandem repeats, which can either be naturally occurring (as in the case of the muscle protein titin) or artificially introduced, leading to a characteristic zig-zag pattern that effectively multiplexes the observation and facilitates identification of properly attached biopolymer chains¹¹⁹. In addition, by chemical modification of the AFM tip, various specific and nonspecific biological interactions can be directly probed⁷².

Measuring mechanochemical force generation

Scope of optical and magnetic tweezers. Force generation by coupling movement with NTP hydrolysis is essential in several biological processes, including the transport of cellular cargo via molecular motors and the enzymatic action of polymerases and helicases. The detailed characterization of kinesins^{120,121} and myosins¹²² by optical tweezers-based force spectroscopy to determine step size, stall force and processivity highlight the breadth of information that can be obtained using single-molecule tools.

Because long DNA can be readily attached to beads, force spectroscopy has also been used to study mechanochemical processes involving nucleic acid-binding proteins. For example, optical tweezers assays have been used to identify the bacteriophage $\Phi 29$ portal motor as one of the strongest biological motors with a stall force of nearly 60 pN during packaging of viral DNA into the capsid¹²³. A particularly challenging biological question that optical tweezers probing has been able to address is that of the mechanism

BOX 2 NEW DEVELOPMENTS INVOLVING SINGLE-MOLECULE FORCE MICROSCOPY

Multidimensional reaction landscapes underlie most biological processes, making it unlikely that a one-dimensional reaction coordinate can fully delineate them. Manipulating multiple interacting molecules in parallel and monitoring multiple observables in one molecule are among the emerging concepts involving force-based single-molecule techniques.

A quad-trap instrument can be generated by first splitting a laser beam into two orthogonally polarized beams, one of which is used to form a continuous trap while the other beam is time-shared over three trap positions using acousto-optic deflectors. The continuous trap is monitored by back-focal-plane interferometry, whereas the other three are used to manipulate trapped biopolymers such as two entangled DNA molecules¹²⁹. Alternatively, holographic images can be used to generate up to 200 optical traps that can be positioned in three dimensions¹³⁰.

Many molecular machines in cells not only generate linear but also rotational force. Measuring torque using optical tweezers can be achieved by using magneto-optical tweezers¹³⁸ or by introducing a small 'rotor' bead to the biomolecule¹⁷. An asymmetric shape or birefringent properties of the trapped particle induce torque upon changing the angular momentum of the trapping light⁶⁴. Hybrid methods can allow the simultaneous measurements of force and torque or force and displacement along multiple axes¹⁷.

Combinations of force with optical single-molecule detection techniques have been realized in several ways. One example is

the merger of atomic force microscopy (AFM) with fluorescence single-molecule microscopy. For combining AFM imaging with confocal microscopy, an infrared light source (850 nm) can be used to detect the position of the cantilever, which minimizes interference with optical detection. A tip-assisted optics system with two scanners facilitates the positioning of the tip within the optical focus¹³⁹. With an AFM-total internal reflection fluorescence microscopy (TIRFM) combination, it is possible to mechanically manipulate a single molecule while monitoring its fluorescence¹⁴⁰.

Hybrids of optical tweezers and single-molecule fluorescence microscopy have recently started to emerge. The intense near-infrared trapping beam of optical tweezers poses as challenges that the much weaker fluorescence emission is overpowered and multiphoton photodamage occurs. To mitigate the problem, three basic solutions have been demonstrated. First, the simultaneous monitoring of mechanical and ligand-binding events in a single myosin molecule has been achieved by physically separating the locations of two trap beams and the TIRFM-generated evanescent field¹²⁵. Second, the unzipping of single 15-base-pair DNA molecules has been induced using optical tweezers and simultaneously has been observed using TIRFM by careful selection of fluorophores and optical filters¹²⁶. Perhaps the most elegant approach is to interlace in time the optical tweezers and TIRFM laser beams to prevent the simultaneous exposure of fluorophores to both lasers¹²⁷.

by which enzymes such as RNA polymerase couple their chemical and mechanical cycles^{12,70}. Furthermore, the incorporation of rotational control into optical or magnetic tweezers has begun to address the question of how biomolecular motors including F_1F_0 ATP synthase, topoisomerases and polymerases generate torque¹⁷.

Scope and limitations of TPM. Prominent applications of TPM have arisen from the single-molecule observation of motor enzymes that shorten or lengthen a tether over time^{61,62}. In a variation of TPM, rotational motions can be visualized through attachment of a bead¹²⁴ or actin filament⁸⁷, although it is difficult to calibrate the drag forces exerted by the latter. TPM is a rather passive technique as it relies on the Brownian motion of a microscopic bead at the end of an invisible single-molecule tether. Artifacts from the presence of multiple tethers can be minimized by using sufficiently small biopolymer:bead ratios and by sorting out beads with asymmetric radial position distributions. Additional challenges arise from spurious tethering and can only be avoided by careful controls and systematic comparisons of samples⁶⁰.

FUTURE TOOLS

The technical advances in single-molecule tools over the past two decades have been staggering. Consequently, whole new fields of biological inquiry have opened up, bringing to life Feynman's vision from half a century ago¹. One remaining limitation of single-molecule tools is the fact that they typically access only a limited number of observables at a time, making an understanding of complex biological processes tedious because many assays have to be developed. The future of single-molecule microscopy will thus increasingly see applications that combine tools, for example, to measure and exert mechanical forces while monitoring in real-time the structural response by single-molecule fluorescence^{12,17} (**Box 2**). Such combinations will be synergistic because optical tweezers, for example, do not reveal precisely where in a macromolecular complex a force is exerted, and single-molecule fluorescence is a passive technique as it cannot favor and probe a specific reaction coordinate. Pioneering efforts that exploit such synergisms to correlate mechanical force with molecular (re)action are still sparse^{125–128} and may need commercialization of instrumentation to reach mainstream biology.

Another route to increased information content and experimental control in single-molecule experiments can be expected from further improvements of individual single-molecule tools. For example, optical tweezers can be multiplexed by controlling arrays of beads through splitting the trapping beam¹²⁹ or through computer-generating holograms with arbitrary three-dimensional light patterns¹³⁰ (**Box 2**). Similarly, single-molecule fluorescence imaging can be multiplexed by the use of improved, narrow-emission fluorophores combined with high-content screening approaches as currently used at the ensemble level in drug discovery. Such approaches may eventually enable 'single-molecule systems biology'. The future of the biosciences is thus illuminated by single-molecule microscopy, a field that is ready for more widespread use.

ACKNOWLEDGMENTS

This work was supported in part by US National Institutes of Health grants GM062357, GM081025 and GM037006, and US National Science Foundation Chemical Bonding Center award 0533019.

Published online at <http://www.nature.com/naturemethods/>
Reprints and permissions information is available online at <http://npg.nature.com/reprintsandpermissions/>

1. Feynman, R.P. in *Miniaturization* (ed., Gilbert, H. D.) 282–296 (Reinhold Publishing Corporation, New York, 1961).
Feynman's now-famous deliberations on the "plenty of room at the bottom" inspired several generations of scientists to seek to fill this room with nanometer-scale materials and techniques to study them.
2. Binning, G., Rohrer, H., Gerber, C. & Weibel, E. Surface studies by scanning tunneling microscopy. *Phys. Rev. Lett.* **49**, 57–61 (1982).
3. Binning, G., Quate, C.F. & Gerber, C. Atomic force microscope. *Phys. Rev. Lett.* **56**, 930–933 (1986).
A demonstration of the concept of atomic force microscopy by the combination of a scanning tunneling microscope and a stylus profilometer that is able to investigate surfaces of insulators on an atomic scale.
4. Pohl, D.W., Denk, W. & Lanz, M. Optical stethoscopy: image recording with resolution $\lambda/20$. *Appl. Phys. Lett.* **44**, 651–653 (1984).
5. Moerner, W.E. & Kador, L. Optical-detection and spectroscopy of single molecules in a solid. *Phys. Rev. Lett.* **62**, 2535–2538 (1989).
Optical absorption spectrum from a single molecule of pentacene in a p-terphenyl crystal at the temperature of liquid helium.
6. Orrit, M. & Bernard, J. Single pentacene molecules detected by fluorescence excitation in a para-terphenyl crystal. *Phys. Rev. Lett.* **65**, 2716–2719 (1990).
Fluorescence detection of single pentacene molecules in a p-terphenyl crystal at low temperature.
7. Moerner, W.E. A dozen years of single-molecule spectroscopy in physics, chemistry, and biophysics. *J. Phys. Chem. B* **106**, 910–927 (2002).
8. Orrit, M. Single-molecule spectroscopy: the road ahead. *J. Chem. Phys.* **117**, 10938–10946 (2002).
9. Shera, E.B., Seitzinger, N.K., Davis, L.M., Keller, R.A. & Soper, S.A. Detection of single fluorescent molecules. *Chem. Phys. Lett.* **174**, 553–557 (1990).
Single-molecule fluorescence detection in solution at room temperature.
10. Dickson, R.M., Norris, D.J., Tzeng, Y.L. & Moerner, W.E. Three-dimensional imaging of single molecules solvated in pores of poly(acrylamide) gels. *Science* **274**, 966–969 (1996).
11. Funatsu, T., Harada, Y., Tokunaga, M., Saito, K. & Yanagida, T. Imaging of single fluorescent molecules and individual ATP turnovers by single myosin molecules in aqueous solution. *Nature* **374**, 555–559 (1995).
A refinement of epi-fluorescence and total internal reflection microscopies to achieve video-rate imaging of single molecules in aqueous solution.
12. Greenleaf, W.J., Woodside, M.T. & Block, S.M. High-resolution, single-molecule measurements of biomolecular motion. *Annu. Rev. Biophys. Biomol. Struct.* **36**, 171–190 (2007).
13. Ditzler, M.A., Aleman, E.A., Rueda, D. & Walter, N.G. Focus on function: single molecule RNA enzymology. *Biopolymers* **87**, 302–316 (2007).
14. Moerner, W.E. New directions in single-molecule imaging and analysis. *Proc. Natl. Acad. Sci. USA* **104**, 12596–12602 (2007).
15. Walter, N.G. *et al.* Under the microscope: single molecule symposium at the University of Michigan, 2006. *Biopolymers* **85**, 106–114 (2007).
16. Selvin, P.R. & Ha, T., eds. *Single-Molecule Techniques: A Laboratory Manual* (Cold Spring Harbor Laboratory Press, Cold Spring Harbor, New York, 2008).
17. Moffitt, J.R., Chemla, Y.R., Smith, S.B. & Bustamante, C. Recent advances in optical tweezers. *Annu. Rev. Biochem.* (in the press) (2008).
18. Neuman, K.C. & Nagy, A. Single-molecule force spectroscopy: optical tweezers, magnetic tweezers and atomic force microscopy. *Nat. Methods* **5**, 491–405 (2008).
19. Roy, R., Hohng, S. & Ha, T. A practical guide to single-molecule FRET. *Nat. Methods* **5**, 507–516 (2008).
20. Harris, T.D. *et al.* Single-molecule DNA sequencing of a viral genome. *Science* **320**, 106–109 (2008).
21. Michalet, X. & Weiss, S. Single-molecule spectroscopy and microscopy. *Compt. Rend. Phys.* **3**, 619–644 (2002).
22. Moerner, W.E. & Fromm, D.P. Methods of single-molecule fluorescence spectroscopy and microscopy. *Rev. Sci. Instrum.* **74**, 3597–3619 (2003).
23. Lakowicz, J.R. *Principles of Fluorescence Spectroscopy*, 3rd edn. (Springer, New York, 2006).
24. Yang, W., Gelles, J. & Musser, S.M. Imaging of single-molecule translocation through nuclear pore complexes. *Proc. Natl. Acad. Sci. USA* **101**, 12887–12892 (2004).
25. Tokunaga, M., Imamoto, N. & Sakata-Sogawa, K. Highly inclined thin illumination enables clear single-molecule imaging in cells. *Nat. Methods* **5**, 159–161 (2008).
26. Conchello, J.A. & Lichtman, J.W. Optical sectioning microscopy. *Nat. Methods* **2**, 920–931 (2005).
27. Kim, H.D. *et al.* Mg^{2+} -dependent conformational change of RNA studied by fluorescence correlation and FRET on immobilized single molecules. *Proc. Natl. Acad. Sci. USA* **99**, 4284–4289 (2002).



28. Axelrod, D. Total internal reflection fluorescence microscopy in cell biology. *Methods Enzymol.* **361**, 1–33 (2003).
29. Levene, M.J. *et al.* Zero-mode waveguides for single-molecule analysis at high concentrations. *Science* **299**, 682–686 (2003).
30. Korlach, J. *et al.* Selective aluminum passivation for targeted immobilization of single DNA polymerase molecules in zero-mode waveguide nanostructures. *Proc. Natl. Acad. Sci. USA* **105**, 1176–1181 (2008).
31. Gorris, H.H., Blicharz, T.M. & Walt, D.R. Optical-fiber bundles. *FEBS J.* **274**, 5462–5470 (2007).
32. Mannion, J.T. & Craighead, H.G. Nanofluidic structures for single biomolecule fluorescent detection. *Biopolymers* **85**, 131–143 (2007).
33. Brewer, L.R. & Bianco, P.R. Laminar flow cells for single-molecule studies of DNA-protein interactions. *Nat. Methods* **5**, 517–525 (2008).
34. Eggeling, C., Fries, J.R., Brand, L., Gunther, R. & Seidel, C.A. Monitoring conformational dynamics of a single molecule by selective fluorescence spectroscopy. *Proc. Natl. Acad. Sci. USA* **95**, 1556–1561 (1998).
35. Lee, T.H. *et al.* Measuring the folding transition time of single RNA molecules. *Biophys. J.* **92**, 3275–3283 (2007).
36. Thompson, R.E., Larson, D.R. & Webb, W.W. Precise nanometer localization analysis for individual fluorescent probes. *Biophys. J.* **82**, 2775–2783 (2002).
37. Yildiz, A. *et al.* Myosin V walks hand-over-hand: single fluorophore imaging with 1.5-nm localization. *Science* **300**, 2061–2065 (2003).
- Single fluorophore tracking refined to nanometer resolution in dynamic biological samples.**
38. Toprak, E. & Selvin, P.R. New fluorescent tools for watching nanometer-scale conformational changes of single molecules. *Annu. Rev. Biophys. Biomol. Struct.* **36**, 349–369 (2007).
39. Park, H., Toprak, E. & Selvin, P.R. Single-molecule fluorescence to study molecular motors. *Q. Rev. Biophys.* **40**, 87–111 (2007).
40. Walter, N.G. Structural dynamics of catalytic RNA highlighted by fluorescence resonance energy transfer. *Methods* **25**, 19–30 (2001).
41. Kapanidis, A.N. & Weiss, S. Fluorescent probes and bioconjugation chemistries for single-molecule fluorescence analysis of biomolecules. *J. Chem. Phys.* **117**, 10953–10964 (2002).
42. Rasnik, I., Mckinney, S.A. & Ha, T. Surfaces and orientations: much to FRET about? *Acc. Chem. Res.* **38**, 542–548 (2005).
43. Yin, J. *et al.* Single-cell FRET imaging of transferrin receptor trafficking dynamics by Sfp-catalyzed, site-specific protein labeling. *Chem. Biol.* **12**, 999–1006 (2005).
44. Hausteiner, E. & Schwille, P. Fluorescence correlation spectroscopy: novel variations of an established technique. *Annu. Rev. Biophys. Biomol. Struct.* **36**, 151–169 (2007).
45. Van Orden, A. & Jung, J. Fluorescence correlation spectroscopy for probing the kinetics and mechanisms of DNA hairpin formation. *Biopolymers* **89**, 1–16 (2008).
46. Michalet, X. & Weiss, S. Using photon statistics to boost microscopy resolution. *Proc. Natl. Acad. Sci. USA* **103**, 4797–4798 (2006).
47. Geerts, H. *et al.* Nanovid tracking: a new automatic method for the study of mobility in living cells based on colloidal gold and video microscopy. *Biophys. J.* **52**, 775–782 (1987).
48. Gelles, J., Schnapp, B.J. & Sheetz, M.P. Tracking kinesin-driven movements with nanometre-scale precision. *Nature* **331**, 450–453 (1988).
- Tracking of nanometer-scale motion in dynamic biological systems by attaching microscopic beads.**
49. Schafer, D.A., Gelles, J., Sheetz, M.P. & Landick, R. Transcription by single molecules of RNA polymerase observed by light-microscopy. *Nature* **352**, 444–448 (1991).
50. Schmidt, T., Schutz, G.J., Baumgartner, W., Gruber, H.J. & Schindler, H. Imaging of single molecule diffusion. *Proc. Natl. Acad. Sci. USA* **93**, 2926–2929 (1996).
51. Ram, S., Ward, E.S. & Ober, R.J. Beyond Rayleigh's criterion: a resolution measure with application to single-molecule microscopy. *Proc. Natl. Acad. Sci. USA* **103**, 4457–4462 (2006).
52. Churchman, L.S., Okten, Z., Rock, R.S., Dawson, J.F. & Spudich, J.A. Single molecule high-resolution colocalization of Cy3 and Cy5 attached to macromolecules measures intramolecular distances through time. *Proc. Natl. Acad. Sci. USA* **102**, 1419–1423 (2005).
53. Gordon, M.P., Ha, T. & Selvin, P.R. Single-molecule high-resolution imaging with photobleaching. *Proc. Natl. Acad. Sci. USA* **101**, 6462–6465 (2004).
54. Qu, X.H., Wu, D., Mets, L. & Scherer, N.F. Nanometer-localized multiple single-molecule fluorescence microscopy. *Proc. Natl. Acad. Sci. USA* **101**, 11298–11303 (2004).
55. Rust, M.J., Bates, M. & Zhuang, X.W. Sub-diffraction-limit imaging by stochastic optical reconstruction microscopy (STORM). *Nat. Methods* **3**, 793–795 (2006).
56. Betzig, E. *et al.* Imaging intracellular fluorescent proteins at nanometer resolution. *Science* **313**, 1642–1645 (2006).
- Imaging of intracellular proteins at nanometer spatial resolution by stochastic photoswitching.**
57. Hess, S.T., Girirajan, T.P.K. & Mason, M.D. Ultra-high resolution imaging by fluorescence photoactivation localization microscopy. *Biophys. J.* **91**, 4258–4272 (2006).
58. Sharonov, A. & Hochstrasser, R.M. Wide-field subdiffraction imaging by accumulated binding of diffusing probes. *Proc. Natl. Acad. Sci. USA* **103**, 18911–18916 (2006).
59. Ashkin, A. Acceleration and trapping of particles by radiation pressure. *Phys. Rev. Lett.* **24**, 156 (1970).
- Optical tweezers implemented as a noninvasive manipulation technique.**
60. Lambert, M.N. *et al.* Mg²⁺-induced compaction of single RNA molecules monitored by tethered particle microscopy. *Biophys. J.* **90**, 3672–3685 (2006).
61. Schafer, D.A., Gelles, J., Sheetz, M.P. & Landick, R. Transcription by single molecules of RNA polymerase observed by light microscopy. *Nature* **352**, 444–448 (1991).
62. Dohoney, K.M. & Gelles, J. Chi-sequence recognition and DNA translocation by single RecBCD helicase/nuclease molecules. *Nature* **409**, 370–374 (2001).
63. van Oijen, A.M. *et al.* Single-molecule kinetics of lambda exonuclease reveal base dependence and dynamic disorder. *Science* **301**, 1235–1238 (2003).
64. La Porta, A. & Wang, M.D. Optical torque wrench: angular trapping, rotation, and torque detection of quartz microparticles. *Phys. Rev. Lett.* **92**, 190801 (2004).
65. Deufel, C., Forth, S., Simmons, C.R., Dejgoshia, S. & Wang, M.D. Nanofabricated quartz cylinders for angular trapping: DNA supercoiling torque detection. *Nat. Methods* **4**, 223–225 (2007).
66. Yang, Y., Wang, H. & Erie, D.A. Quantitative characterization of biomolecular assemblies and interactions using atomic force microscopy. *Methods* **29**, 175–187 (2003).
67. Weber, P.C., Ohlendorf, D.H., Wendoloski, J.J. & Salemme, F.R. Structural origins of high-affinity biotin binding to streptavidin. *Science* **243**, 85–88 (1989).
68. Fan, F.R. & Bard, A.J. Electrochemical detection of single molecules. *Science* **267**, 871–874 (1995).
69. Hla, S.W. & Rieder, K.H. STM control of chemical reaction: single-molecule synthesis. *Annu. Rev. Phys. Chem.* **54**, 307–330 (2003).
70. Abbondanzieri, E.A., Greenleaf, W.J., Shaevitz, J.W., Landick, R. & Block, S.M. Direct observation of base-pair stepping by RNA polymerase. *Nature* **438**, 460–465 (2005).
- The authors show that Ångstrom resolution can be obtained using ultrasensitive optical tweezers to observe single steps of RNA polymerase along a double-stranded DNA template.**
71. Charvin, G., Strick, T.R., Bensimon, D. & Croquette, V. Tracking topoisomerase activity at the single-molecule level. *Annu. Rev. Biophys. Biomol. Struct.* **34**, 201–219 (2005).
72. Kedrov, A., Janovjak, H., Sapra, K.T. & Muller, D.J. Deciphering molecular interactions of native membrane proteins by single-molecule force spectroscopy. *Annu. Rev. Biophys. Biomol. Struct.* **36**, 233–260 (2007).
73. Ke, Y., Lindsay, S., Chang, Y., Liu, Y. & Yan, H. Self-assembled water-soluble nucleic acid probe tiles for label-free RNA hybridization assays. *Science* **319**, 180–183 (2008).
74. Michalet, X. *et al.* The power and prospects of fluorescence microscopies and spectroscopies. *Annu. Rev. Biophys. Biomol. Struct.* **32**, 161–182 (2003).
75. Tinnefeld, P. & Sauer, M. Branching out of single-molecule fluorescence spectroscopy: challenges for chemistry and influence on biology. *Angew. Chem. Int. Edn. Engl.* **44**, 2642–2671 (2005).
76. Thompson, N.L., Lieto, A.M. & Allen, N.W. Recent advances in fluorescence correlation spectroscopy. *Curr. Opin. Struct. Biol.* **12**, 634–641 (2002).
77. Elson, E.L. Quick tour of fluorescence correlation spectroscopy from its inception. *J. Biomed. Opt.* **9**, 857–864 (2004).
78. Leake, M.C. *et al.* Stoichiometry and turnover in single, functioning membrane protein complexes. *Nature* **443**, 355–358 (2006).
79. Shu, D., Zhang, H., Jin, J. & Guo, P. Counting of six pRNAs of phi29 DNA-packaging motor with customized single-molecule dual-view system. *EMBO J.* **26**, 527–537 (2007).
80. Armani, A.M., Kulkarni, R.P., Fraser, S.E., Flagan, R.C. & Vahala, K.J. Label-free, single-molecule detection with optical microcavities. *Science* **317**, 783–787 (2007).
81. Huang, B. *et al.* Counting low-copy number proteins in a single cell. *Science* **315**, 81–84 (2007).
82. Zhuang, X. Single-molecule RNA science. *Annu. Rev. Biophys. Biomol. Struct.* **34**, 399–414 (2005).

83. Cosa, G. *et al.* Secondary structure and secondary structure dynamics of DNA hairpins complexed with HIV-1 NC protein. *Biophys. J.* **87**, 2759–2767 (2004).
84. Wang, D. & Geva, E. Protein structure and dynamics from single-molecule fluorescence resonance energy transfer. *J. Phys. Chem. B* **109**, 1626–1634 (2005).
85. Yang, H. *et al.* Protein conformational dynamics probed by single-molecule electron transfer. *Science* **302**, 262–266 (2003).
86. Reinhard, B.M., Sheikholeslami, S., Mastroianni, A., Alivisatos, A.P. & Liphardt, J. Use of plasmon coupling to reveal the dynamics of DNA bending and cleavage by single EcoRV restriction enzymes. *Proc. Natl. Acad. Sci. USA* **104**, 2667–2672 (2007).
87. Noji, H., Yasuda, R., Yoshida, M. & Kinosita, K. Direct observation of the rotation of F-1-ATPase. *Nature* **386**, 299–302 (1997).
88. Zhuang, X.W. *et al.* Correlating structural dynamics and function in single ribozyme molecules. *Science* **296**, 1473–1476 (2002).
- A detailed study of the hairpin ribozyme reveals profound molecular heterogeneities in single biomolecules that is largely lost in the ensemble average.**
89. Rueda, D. *et al.* Single-molecule enzymology of RNA: essential functional groups impact catalysis from a distance. *Proc. Natl. Acad. Sci. USA* **101**, 10066–10071 (2004).
90. Nahas, M.K. *et al.* Observation of internal cleavage and ligation reactions of a ribozyme. *Nat. Struct. Mol. Biol.* **11**, 1107–1113 (2004).
91. Liu, S., Bokinsky, G., Walter, N.G. & Zhuang, X. Dissecting the multistep reaction pathway of an RNA enzyme by single-molecule kinetic “fingerprinting”. *Proc. Natl. Acad. Sci. USA* **104**, 12634–12639 (2007).
92. Kapanidis, A.N. *et al.* Initial transcription by RNA polymerase proceeds through a DNA-scrunching mechanism. *Science* **314**, 1144–1147 (2006).
93. Myong, S., Rasnik, I., Joo, C., Lohman, T.M. & Ha, T. Repetitive shuttling of a motor protein on DNA. *Nature* **437**, 1321–1325 (2005).
94. Lu, H.P., Xun, L. & Xie, X.S. Single molecule enzymatic dynamics. *Science* **282**, 1877–1882 (1998).
95. Blanchard, S.C., Gonzalez, R.L., Kim, H.D., Chu, S. & Puglisi, J.D. tRNA selection and kinetic proofreading in translation. *Nat. Struct. Mol. Biol.* **11**, 1008–1014 (2004).
96. English, B.P. *et al.* Ever-fluctuating single enzyme molecules: Michaelis-Menten equation revisited. *Nat. Chem. Biol.* **2**, 87–94 (2006).
97. Luo, G., Wang, M., Konigsberg, W.H. & Xie, X.S. Single-molecule and ensemble fluorescence assays for a functionally important conformational change in T7 DNA polymerase. *Proc. Natl. Acad. Sci. USA* **104**, 12610–12615 (2007).
98. Bustamante, C., Bryant, Z. & Smith, S. B. Ten years of tension: single-molecule DNA mechanics. *Nature* **421**, 423–427 (2003).
99. Rotman, B. Measurement of activity of single molecules of beta-D-galactosidase. *Proc. Natl. Acad. Sci. USA* **47**, 1981–1991 (1961).
100. Xue, Q.F. & Yeung, E.S. Differences in the chemical-reactivity of individual molecules of an enzyme. *Nature* **373**, 681–683 (1995).
101. Laurence, T.A., Kong, X., Jager, M. & Weiss, S. Probing structural heterogeneities and fluctuations of nucleic acids and denatured proteins. *Proc. Natl. Acad. Sci. USA* **102**, 17348–17353 (2005).
102. Lee, N.K., Koh, H.R., Han, K.Y. & Kim, S.K. Folding of 8–17 deoxyribozyme studied by three-color alternating-laser excitation of single molecules. *J. Am. Chem. Soc.* **129**, 15526–15534 (2007).
103. Liu, R., Hu, D., Tan, X. & Lu, H.P. Revealing two-state protein-protein interactions of calmodulin by single-molecule spectroscopy. *J. Am. Chem. Soc.* **128**, 10034–10042 (2006).
104. Zhuang, X. *et al.* A single-molecule study of RNA catalysis and folding. *Science* **288**, 2048–2051 (2000).
105. Dorywalska, M. *et al.* Site-specific labeling of the ribosome for single-molecule spectroscopy. *Nucleic Acids Res.* **33**, 182–189 (2005).
106. Bacia, K., Kim, S.A. & Schwille, P. Fluorescence cross-correlation spectroscopy in living cells. *Nat. Methods* **3**, 83–89 (2006).
107. Murakoshi, H. *et al.* Single-molecule imaging analysis of Ras activation in living cells. *Proc. Natl. Acad. Sci. USA* **101**, 7317–7322 (2004).
108. Elf, J., Li, G.W. & Xie, X.S. Probing transcription factor dynamics at the single-molecule level in a living cell. *Science* **316**, 1191–1194 (2007).
109. Xie, X.S., Yu, J. & Yang, W.Y. Living cells as test tubes. *Science* **312**, 228–230 (2006).
110. Rueda, D. & Walter, N.G. Single molecule fluorescence control for nanotechnology. *J. Nanosci. Nanotechnol.* **5**, 1990–2000 (2005).
111. Huang, B., Wang, W., Bates, M. & Zhuang, X. Three-dimensional super-resolution imaging by stochastic optical reconstruction microscopy. *Science* **319**, 810–813 (2008).
112. Geisler, C. *et al.* Resolution of lambda/10 in fluorescence microscopy using fast single molecule photo-switching. *Appl. Phys. A* **88**, 223–226 (2007).
113. Bock, H. *et al.* Two-color far-field fluorescence nanoscopy based on photoswitchable emitters. *Appl. Phys. B* **88**, 161–165 (2007).
114. Manley, S. *et al.* High-density mapping of single-molecule trajectories with photoactivated localization microscopy. *Nat. Methods* **5**, 155–157 (2008).
115. Hell, S.W. Far-field optical nanoscopy. *Science* **316**, 1153–1158 (2007).
116. Donnert, G. *et al.* Two-color far-field fluorescence nanoscopy. *Biophys. J.* **92**, L67–L69 (2007).
117. Willig, K.I., Harke, B., Medda, R. & Hell, S.W. STED microscopy with continuous wave beams. *Nat. Methods* **4**, 915–918 (2007).
118. Collin, D. *et al.* Verification of the Crooks fluctuation theorem and recovery of RNA folding free energies. *Nature* **437**, 231–234 (2005).
119. Carrion-Vazquez, M. *et al.* The mechanical stability of ubiquitin is linkage dependent. *Nat. Struct. Biol.* **10**, 674–676 (2003).
120. Block, S.M., Goldstein, L.S. & Schnapp, B.J. Bead movement by single kinesin molecules studied with optical tweezers. *Nature* **348**, 348–352 (1990).
121. Kuo, S.C. & Sheetz, M.P. Force of single kinesin molecules measured with optical tweezers. *Science* **260**, 232–234 (1993).
122. Nishizaka, T., Miyata, H., Yoshikawa, H., Ishiwata, S. & Kinosita, K., Jr. Unbinding force of a single motor molecule of muscle measured using optical tweezers. *Nature* **377**, 251–254 (1995).
123. Smith, D.E. *et al.* The bacteriophage straight phi29 portal motor can package DNA against a large internal force. *Nature* **413**, 748–752 (2001).
124. Sowa, Y. *et al.* Direct observation of steps in rotation of the bacterial flagellar motor. *Nature* **437**, 916–919 (2005).
125. Ishijima, A. *et al.* Simultaneous observation of individual ATPase and mechanical events by a single myosin molecule during interaction with actin. *Cell* **92**, 161–171 (1998).
- Combination of single-molecule fluorescence microscopy with optical tweezers.**
126. Lang, M.J., Fordyce, P.M., Engh, A.M., Neuman, K.C. & Block, S.M. Simultaneous, coincident optical trapping and single-molecule fluorescence. *Nat. Methods* **1**, 133–139 (2004).
127. Brau, R.R., Tarsa, P.B., Ferrer, J.M., Lee, P. & Lang, M.J. Interlaced optical force-fluorescence measurements for single molecule biophysics. *Biophys. J.* **91**, 1069–1077 (2006).
128. Hohng, S. *et al.* Fluorescence-force spectroscopy maps two-dimensional reaction landscape of the Holliday junction. *Science* **318**, 279–283 (2007).
129. Noom, M.C., van den Broek, B., van Mameren, J. & Wuite, G.J. Visualizing single DNA-bound proteins using DNA as a scanning probe. *Nat. Methods* **4**, 1031–1036 (2007).
130. Grier, D.G. & Roichman, Y. Holographic optical trapping. *Appl. Opt.* **45**, 880–887 (2006).
131. Kask, P., Palo, K., Ullmann, D. & Gall, K. Fluorescence-intensity distribution analysis and its application in biomolecular detection technology. *Proc. Natl. Acad. Sci. USA* **96**, 13756–13761 (1999).
132. Cox, I.J., Sheppard, C.J.R. & Wilson, T. Super-resolution by confocal fluorescent microscopy. *Optik* **60**, 391–396 (1982).
133. Edidin, M. Near-field scanning optical microscopy, a siren call to biology. *Traffic* **2**, 797–803 (2001).
134. Chen, Y., Muller, J.D., So, P.T.C. & Gratton, E. The photon counting histogram in fluorescence fluctuation spectroscopy. *Biophys. J.* **77**, 553–567 (1999).
135. Heintzmann, R., Jovin, T.M. & Cremer, C. Saturated patterned excitation microscopy - a concept for optical resolution improvement. *J. Opt. Soc. Am.* **19**, 1599–1609 (2002).
136. Gustafsson, M.G.L. Nonlinear structured-illumination microscopy: wide-field fluorescence imaging with theoretically unlimited resolution. *Proc. Natl. Acad. Sci. USA* **102**, 13081–13086 (2005).
137. Hell, S.W. & Wichmann, J. Breaking the diffraction resolution limit by stimulated-emission: stimulated-emission-depletion fluorescence microscopy. *Opt. Lett.* **19**, 780–782 (1994).
- The authors present the concept of stimulated emission depletion fluorescence microscopy to break Abbe's diffraction limit.**
138. Crut, A., Koster, D.A., Seidel, R., Wiggins, C.H. & Dekker, N.H. Fast dynamics of supercoiled DNA revealed by single-molecule experiments. *Proc. Natl. Acad. Sci. USA* **104**, 11957–11962 (2007).
139. Owen, R.J., Heyes, C.D., Knebel, D., Rocker, C. & Nienhaus, G.U. An integrated instrumental setup for the combination of atomic force microscopy with optical spectroscopy. *Biopolymers* **82**, 410–414 (2006).
140. Hugel, T. *et al.* Single-molecule optomechanical cycle. *Science* **296**, 1103–1106 (2002).